Available online at www.sciencedirect.com
ScienceDirect
Ceramics International 35 (2009) 1211–1218
CERAMICS INTERNATIONAL
www.elsevier.com/locate/ceramint

Preparation and characterization of some multicomponent silicate glasses and their glass–ceramics derivatives for dental applications

Fatma H. ElBatal [a,*], Moenis A. Azooz [a], Yousry M. Hamdy [b]

[a] Glass Research Department, National Research Center, Dokki, Cairo, Egypt
[b] Spectroscopy Department, National Research Center, Dokki, Cairo, Egypt

Received 9 April 2008; received in revised form 14 May 2008; accepted 13 June 2008
Available online 22 July 2008

Abstract

The chemical corrosion and UV–vis absorption and infrared absorption spectra of binary and multicomponent lithium silicate glasses and corresponding glass–ceramics were investigated. The chemical durability of the glasses and derived glass–ceramics was found to be excellent to all leaching media. The IR absorption spectra of the glass and glass–ceramic samples reveal absorption bands of characteristic groups mainly due to major silicate network besides the possible sharing of network units due to some involving oxide constituents. X-ray analysis of glass–ceramics indicates the separation of lithium disilicate phase as the main constituent beside other phases according to the specimen chemical constituents. The obvious promising investigated chemical and physical properties are correlated with the presence of multioxides such as Al_2O_3, TiO_2, MgO and ZrO_2. Transmission and reflectivity properties reveal acceptable data. The prepared glass–ceramics are recommended for dental applications.

Keywords: B. Electron microscopy; B. Spectroscopy; C. Corrosion; D. Glass ceramics; E. Biomedical applications

1. Introduction

In the development of biocompatible and bioactive glass–ceramics for medical use, two different types of materials can be recognized that differ in their applications environment and preferred properties [1]. These are materials for use in implantology (medical protheses) and materials used in restorative dentistry (dental protheses). The first group includes bioactive glass–ceramics which form a biologically active hydroxyl-apatite layer that permits chemical bonding with bone and even with soft tissue. Depending on the application of the bioactive glass–ceramic material, it may be load-bearing or not and may need to fulfill special requirements with respect to the bending strength, toughness and Young's modulus. Special optical properties such as translucency and colour are not important in the development of this type of bioactive material.

With regard to glass–ceramic for restorative dental applications, the situation is different [1]. These materials must also fulfill the standards for biomaterial use, such as compatibility with the oral environment. Bioactivity on the surface of the dental restorations, however, must not occur. More importantly, the surface properties of the glass–ceramics, such as shade, translucency, and toughness must correspond to those of natural teeth. Even higher standards are placed on the chemical durability of the material compared with that of natural teeth, since cavities should not occur in the new glass–ceramics.

Glass–ceramics with controlled desirable mechanical and chemical properties and esthetic qualities are used for dental prosthetic applications. One of the first systems developed was based on Li_2O–ZnO–SiO_2 compositions, and subsequent systems based on leucite and mica phases have been developed for dental restorations [2]. These first materials often possessed relatively low strengths that proved problematic for use in highly stresses dental restorations. Recent compositional modifications to lithium disilicate (LS_2) base glasses have yielded translucent glass–ceramics that are characterized by high strength, excellent chemical durability, and the esthetic appearance of natural teeth [3]. An interesting property of these LS_2 glass–ceramics is the high flexural strength due to an unusual microstructure that consists of plate-like crystals of lithium disilicate ($Li_2Si_2O_5$) that are randomly oriented to cause cracks to blunt or branch [1]. The formation of a trisient phase of Li_3PO_4 crystals is assumed to precede the crystallization of the desired LS_2 phases [4].

---

* Corresponding author. Tel.: +20 233335971; fax: +20 233370931.
E-mail address: fh_elbatal@yahoo.co.uk (F.H. ElBatal).

0272-8842/$34.00 © 2008 Elsevier Ltd and Techna Group S.r.l. All rights reserved.
doi:10.1016/j.ceramint.2008.06.009

One important parameter for the design and manufacture of glass–ceramics for dental restorations is the development of a material that reproduces the visible appearance of natural teeth, including colour, translucency and fluorescence properties. The desirable translucency in LS_2 glass–ceramics is achieved by the control of the relative refractive indices and volume concentrations of the crystalline and residual glassy phases [2], whereas colour and fluorescence are achieved by the addition of transition metal oxides and rare-earth oxides, respectively, in the glass composition.

The main objective of this work is to prepare and investigate crystallization behavior and chemical properties of some multicomponent lithium silicate glasses containing some additives like K_2O, Al_2O_3, MgO, CaO, ZrO_2, ZnO or TiO_2 and their corresponding glass–ceramics. The work is extended to study the infrared spectra of the parent glasses and corresponding glass–ceramics to reveal and characterize their structural main building units. Also, absorption spectra of the parent glasses and reflection spectra of their glass–ceramics derivatives were measured.

2. Experimental details

2.1. Preparation of dental glasses

The dental patented [3,5] glass of the basic composition: SiO_2 72.41, Li_2O 15.03 with some additives of K_2O, Al_2O_3, P_2O_5, MgO and ZrO_2 and some other substituted glasses with the compositions shown in Table 1 have been prepared using the normal melting and annealing technique. The materials used in the present investigation for the preparation of the parent glasses were of chemically pure grade. The materials used include fine-grained quartz for silica. Lithia, potash, magnesia, lime were introduced in the form of their respective anhydrous carbonates. TiO_2, ZrO_2, Al_2O_3 and ZnO were added as such. P_2O_5 was added in the form of ammonium dihydrogen phosphate. The weighed batch mixture was melted in platinum crucibles for 2 h after the last traces of the batch materials had disappeared. The melting was carried in an electric furnace at 1400 ± 10 °C. The melt was stirred before casting two or three times in order to achieve a homogeneous melt. Then, the homogenized melt was cast into a preheated stainless steel mould of 1 cm × 0.5 cm × 4 cm dimension. The prepared glasses were removed from the mould and transferred to an annealing muffle furnace regulated at about 450 °C and after 1 h the muffle was left to cool to room temperature at a rate of 25 °C/h. It was found profitable to prepare two references of a binary lithium disilicate glass and a ternary lithium aluminum silicate glass for comparative study.

Table 2
Heat treatment regime used to produce corresponding glass–ceramics

Glass sample no.	First nucleation temperature (°C)	Second crystal growth temperature (°C)
1	650	850
2	600	800
3	600	800
4	600	850
5	580	800
6	600	850
7	600	800
8	600	800
9	600	800
10	600	850
11	600	850

2.2. Differential thermal analysis

Differential thermal analysis (DTA) measurement was carried out on powdered glass samples which were examined up to 1000 °C using a powdered alumina as a reference material. A DTA PerkinElmer DTA-7 apparatus was used in this study. The DTA data were used to find out the proper heat treatment temperatures to obtain the appropriate glass–ceramic derivatives with high crystallinity. Briefly, the values obtained for glass nucleation temperature and the onset of crystallization temperature are given in Table 2.

2.3. Heat-treatment regime (conversion to glass–ceramic)

The glass samples were thermally heated in two-step regime at the mentioned temperatures. Each glass was heated slowly to the first nucleation temperature for the formation of sufficient nuclei sites and after holding for 3 h, was then further heated or raised to reach the second chosen crystal growth temperature, and after a second hold for 3 h, the specimen was left to cool inside the muffle furnace to room temperature at a rate of 20 °C/h.

Table 1
Composition of the samples (wt.%)

Sample	SiO_2	Li_2O	K_2O	Al_2O_3	P_2O_5	MgO	ZrO_2	CaO	TiO_2	ZnO
1	72.41	15.03	3.81	3.45	3.92	0.15	1.84	–	–	–
2	70.00	15.03	3.81	3.45	6.33	0.15	1.84	–	–	–
3	70.00	15.03	3.81	3.45	3.16	0.15	1.84	3.16	–	–
4	70.00	12.03	3.81	3.45	3.16	0.15	1.84	6.16	–	–
5	70.00	12.03	3.81	3.45	6.16	0.15	1.84	3.16	–	–
6	70.00	9.03	3.81	3.45	6.16	0.15	1.84	6.16	–	–
7	70.00	15.03	3.81	3.45	3.90	0.15	1.84	–	–	3.16
8	70.00	13.50	3.81	3.45	3.90	0.15	1.84	–	–	4.50
9	70.00	11.50	3.81	–	3.90	0.15	1.84	–	–	6.50
10	70.00	15.03	3.81	3.45	3.90	0.15	1.84	–	3.16	–
11	70.00	13.50	3.81	3.45	3.90	0.15	1.84	–	4.50	–

Table 3
Infrared bands position and their assignment

Peak position (cm^{-1})	Assignment
450–480	Bending vibrations of Si–O–Si linkages
600–650	Si–O–Si and O–Si–O bending modes
725–800	Symmetric stretching vibrations of O–Si–O bonds
900–930	Vibrations of non-bridging oxygens or $Si–O^-$ stretching vibrations
1050–1120	Antisymmetric stretching vibrations of bridging oxygens or Si–O–Si stretching vibrations
1400–1460	Carbonate group vibrations
1600–1640	Molecular water vibrations

2.4. X-ray diffraction measurement

The heat-treated glass–ceramics were analyzed by X-ray diffraction in order to identify the crystalline phases that precipitated within the samples during the two-step thermal heat-treatment regime. The samples were ground and the fine powder was examined using a diffractometer adopting Ni-filter and Cu-target. The X-ray diffraction patterns were checked and identified using a Philips PW 1390 X-ray diffractometer.

2.5. Structural analysis of bioglass and bioglass–ceramics

Infrared absorption spectra of the bioglasses and their glass–ceramic derivatives were measured at room temperature (~20 °C) in the wavenumber range of 2000–400 cm^{-1} using a Fourier Transform infrared spectrometer (type Jasco FT-IR, Japan). Fine powders of the samples were mixed with KBr powder in the ratio 1:100 and the mixtures were subjected to a load of 5 tons/cm^2 in an evacuble die to produce clear homogeneous disc. Then, the IR absorption spectra were immediately measured after preparing the disc.

2.6. Chemical corrosion studies

The chemical durability of the prepared bioglasses and their corresponding glass–ceramics were carried out using the grain method which was adopted by several authors [6–9]. Glass grains (0.30–0.60 mm in diameter) were immersed in the respective leaching solution for 1 or 16 h at 80 °C. The applied investigated solutions include 4 vol.% acetic acid as recommended with ISO dental standard 6872 [8], 0.1 M HCl, 0.1 M NaOH and bidistilled water for complete evaluation in acidic, alkaline and neutral solutions.

1 g of the sample grains was placed in a sintered glass crucible G4 which was placed in a 250 ml polyethylene beaker situated in the water bath regulated at 80 °C. 150 ml of the leach solution was introduced to cover the grains. After 1 h, the beaker was removed from the bath and the sintered glass crucible was fitted on a suction pump and the whole solution was pumped through it. The sintered glass crucible was transferred to an air oven at 120 °C for 1 h. Then, the crucible with its content was reweighed and the total loss was calculated. An empty sintered glass crucible G4 was subjected to the same corrosion test and the obtained data were taken into consideration.

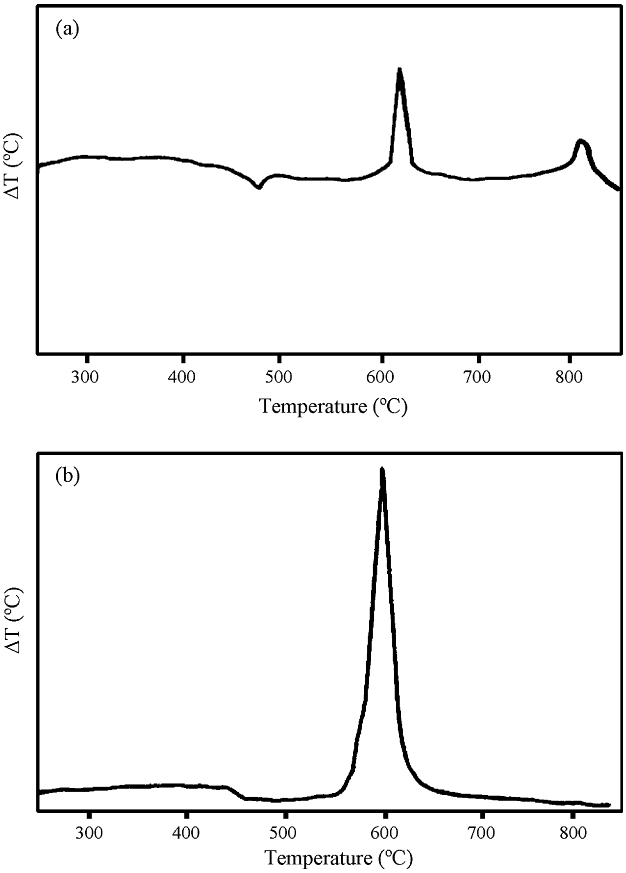

Fig. 1. DTA of base lithium silicate glass and multicomponent sample no. (1).

2.7. UV–vis absorption spectroscopy

Glass samples were ground and highly polished and the thickness of the samples varied around 2.0 ± 0.1 mm. Absorption spectra were collected with a spectrophotometer (type Jasco Corp., V-570, Rel-00, Japan) covering the range from 200 to 1000 nm.

3. Results

3.1. Differential thermal analysis

Fig. 1 illustrates the DTA measurements of both two samples representing a base binary lithium silicate and the multicomponent dental composition (glass no. 3). The DTA curve for binary lithium silicate glass reveals the glass transition temperature (T_g) at about 456 °C and also it is evident a very sharp exothermic peak at about 590 °C. The multicomponent glass DTA curve shows a T_g at 495 °C and also it is obvious two exotherms at about 640 °C and at about 840 °C.

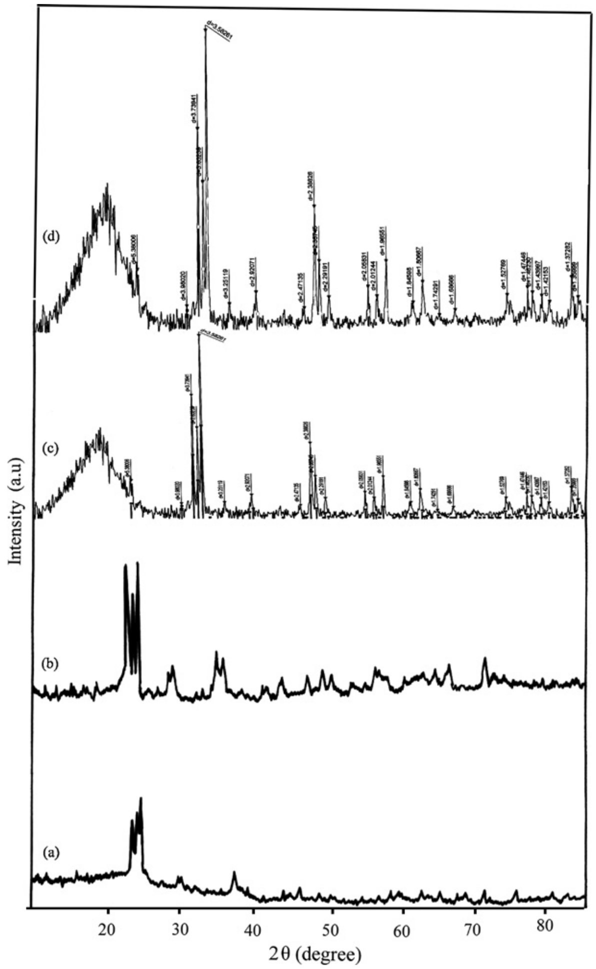

Fig. 2. X-ray diffraction patterns of base LiS_2 glass–ceramic and multicomponent glass–ceramics.

3.2. X-ray diffraction patterns data

Fig. 2 shows the X-ray diffraction patterns for the two references binary lithium silicate and binary lithium aluminium silicate glass–ceramic and the glass–ceramic obtained from the crystallization process of the multicomponent glass no. 3 as a representative for the dental glasses. It is obvious that the glass–ceramics reveal diffraction patterns due to the appearance of crystalline lithium disilicate phase beside the appearance of two other phases in the multicomponent dental sample due to beta-cristobalite and mixed magnesium zirconium oxide solid phase. Careful inspection of the diffraction patterns indicates that the peak intensities of the crystalline phases show variations with the change in the basic glass compositions.

3.3. Infrared spectra of the studied glasses

Fig. 3 illustrates the infrared absorption spectra of the lithium silicate and lithium aluminium silicate together with that due to multicomponent silicate glasses and the results can be summarized as follows:

(a) The absorption frequencies are comparable to the IR spectra usually obtained from traditional silicate glasses.

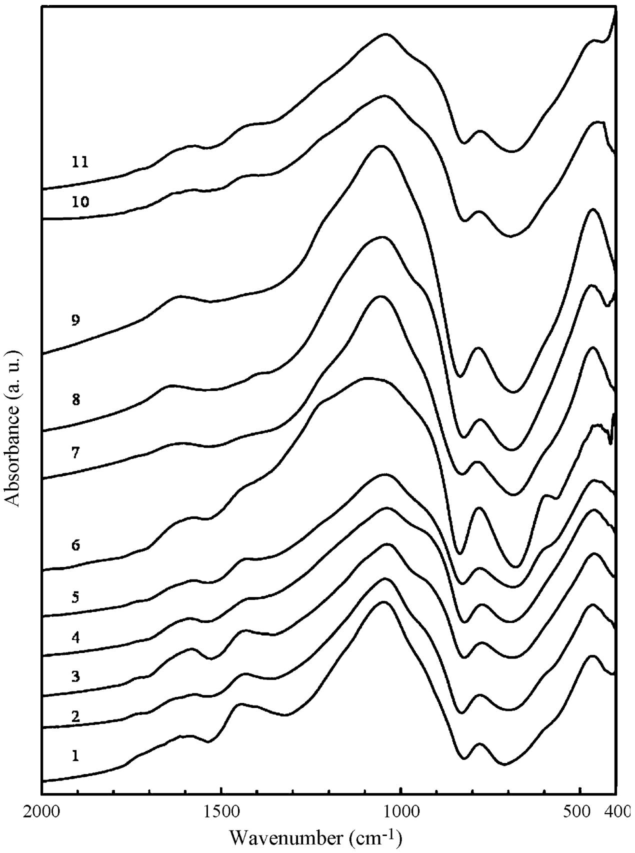

Fig. 3. Infrared absorption spectra of base glasses and multicomponent glasses.

(b) The principal bands are mainly concentrated in the mid region (2000–400) cm^{-1} comprising the main vibrations due to silicate chains. The absorption frequencies are visualized at about 450–460, 730–760, 860, 900–1100, 1430–1480 and 1640 cm^{-1}.

(c) The change in glass composition is observed to cause minor changes in the IR spectra. This can be represented by the observed splitting of the first broad band at about 460 cm^{-1} into component peaks at 400–440 cm^{-1} and the quite resolution of the band at about 720 cm^{-1} and splitting of the second broad band at 900–1100 cm^{-1} into three component peaks. It is evident that the main bands due to silicate chains remain prominent allover the entire samples investigated.

3.4. Infrared absorption of the glass–ceramic derivatives

Fig. 4 illustrates the IR absorption spectra of the corresponding glass–ceramic derivatives from which it can be seen that:

(a) The IR spectra show well-defined highly resolved absorption bands especially in the mid region extending from 400 to 1500 cm^{-1}. This specific region is known to reveal the characteristic vibrations of the silicate chains due to the presence of SiO_2 as the main glass-forming component besides the possible sharing of any of the oxides which can be involved in the network, namely, P_2O_5 and Al_2O_3.

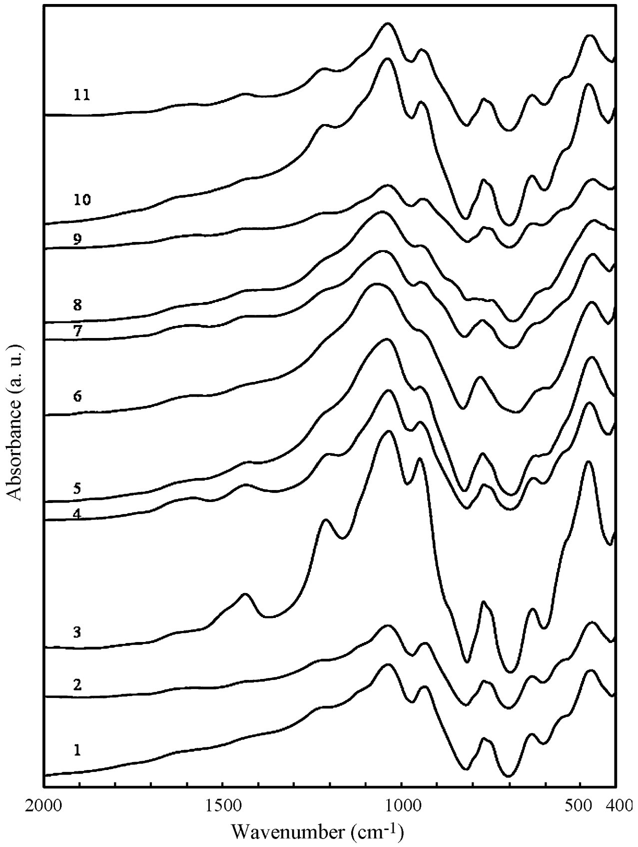

Fig. 4. Infrared absorption spectra of corresponding glass–ceramics.

(b) It is evident that about 14 IR sharp consecutive bands are quite resolved and located at about 405–415, 472–475, 550–555, 635–638, 755–757, 784–786, 850, 935–941, 962, 1025–1030, 1105–1108, 1214–1240, 1430–1450, 1640 cm^{-1}.

(c) It is also obvious that the minor changes in the basic glasses compositions cause some few alterations in the bands positions or intensities.

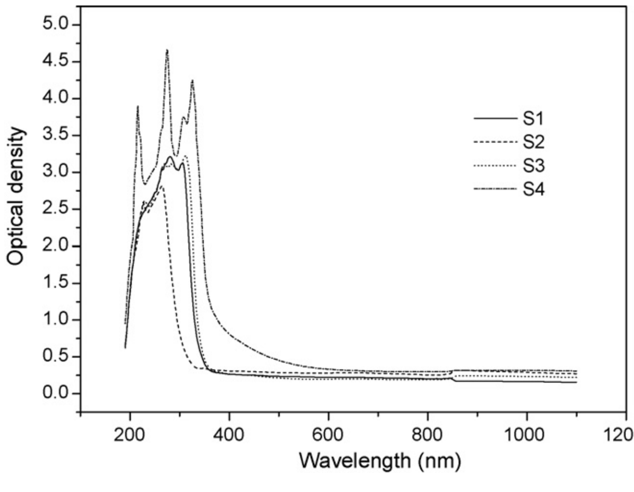

Fig. 5. Absorption spectra of some selected base and multicomponent lithium silicate glasses (S1: sample no. 1, S2: sample no. 2, S3: sample no. 3, S4: sample no. 4).

3.5. *Chemical corrosion of the studied glasses and glass–ceramics derivatives*

The corrosion weight loss with NaOH solution (0.1 M) ranged from 0.01% to 0.03% for glasses and from 0.01% to 0.11% for glass–ceramics.

With distilled water, the corrosion values ranged from 0.01% to 0.04% for glasses and from 0.01% to 0.02% for glass–ceramics. The corrosion weight loss with HCl solution (0.1 M) ranged from 0.03% to 0.06% for glasses and from 0.01% to 0.05% for glass–ceramics. With acetic acid solution (4 vol.%), the corrosion values ranged from 0.01% to 0.03% for glasses and from 0.01% to 0.02% for glass–ceramics.

The results obtained from corrosion studied of the glasses and their corresponding glass–ceramics show that:

(1) The corrosion of all the studied glasses reveal minor or almost no weight loss percents for the action of distilled water or the two acidic solutions, namely HCl or acetic acidic solutions.
(2) The glass–ceramic samples show the same behaviour indicating that such compositions possess excellent chemical durabilities.

3.6. *UV–vis absorption characteristics*

Fig. 5 reveals the absorption curves of some selected glasses including the base lithium aluminum silicate and a multicomponent dental glass and a glass with high TiO_2 content (10%). It is obvious that the base LiAlSi glass and the multicomponent dental glasses show the same sharp ultraviolet charge transfer absorption constituting mostly of three peaks at about 210, 270 and 310 nm while the glass containing high TiO_2 content (10%) reveals somewhat extended absorption with four sharp peaks at about 210, 310, 350 and 380 nm.

4. Discussion

4.1. *Interpretation of the infrared spectra of glasses and corresponding glass–ceramics*

It is obvious that the studied glasses are composed of silica as the main component constituting the SiO_4 backbone network and $Li_2O + K_2O$ act as modifier oxides. Also, the glass contains some other oxides such as Al_2O_3, P_2O_5, MgO, ZrO_2, and TiO_2 in different minor percents which are believed to be able to behave mostly as network forming oxides.

The glasses reveal specific repetitive IR absorption bands extending as illustrated in all the measured regions of infrared spectrum. It is generally accepted that the building units of silicate glasses are SiO_4 tetrahedral network and this postulation is supported by the general close similarity of the infrared spectra with the infrared of the crystalline silicates. It is assumed that in silicate glasses, the SiO_4 tetrahedra are linked at the vertices to form a network, while the various modifiers such as alkali and alkaline earth ions occupy interstices in the network [10]. These prescribed features of glass structure are a straightforward generalization of the structure of crystalline silicates as well which is supported by X-ray diffraction analysis [10–14]. However, the proposed structure of the glassy lithium disilicate composition consists of non-periodic or disordered SiO_4 units. In the glassy state, different units have somewhat different structures or configurations hence they vibrate at slightly different frequencies. When all these frequencies are superimposed, the spectrum and the peaks are observed to be broad and not very sharp as in crystalline analogues. It is important to mention that the general nature of the normal modes of vibration is not greatly altered by the disorder, so that strong modes of vibrations remain strong and weak modes remain weak.

Therefore, the infrared spectra results can be interpreted on the following basis:

(a) IR modes at 800–1200 cm^{-1} are assigned to the asymmetric and symmetric stretching vibrations of the tetrahedral silicate network [10–12].
(b) The IR maxima near 450–600 cm^{-1} have been assigned to bending and rocking motions of the silicate network [10–12].
(c) The IR bands around 1450 cm^{-1} and around 1640 cm^{-1} are related to carbonate groups and molecular water respectively [10,12].
(d) The shift of the bands frequencies to higher or lower wavenumbers can be correlated with the degree of polymerization of the network structure [10] (e.g. by introducing additional new network-forming units, such as PO_4, AlO_4, MgO_4).
(e) The appearance of sharp and splitted peaks in the glass–ceramic samples can be related to the fine-grained and full crystallinity of these samples, after the controlled crystallization process.

Table 3 introduces the observed absorption bands in the studied glasses and glass–ceramics and their assignments together with references.

4.2. Interpretation of the chemical corrosion data

It is generally accepted that the corrosion of silicate glasses by aqueous solutions involves hydration and ion-exchange processes between the alkali modifiers from the glass and hydrogen or hydronium ions from the contact solutions [15–17]. On continuous corrosion, the leaching of alkali ions from the glasses leaves a surface silica-rich layer containing hydrated micropores and leads to an increase in the surface area of the glass in contact with the corrosion solution.

The corrosion of patented Hench's bioglass is agreed upon [15,18,19] to be rapid than traditional commercial silicate glasses due to the presence of substantial amounts of both alkali oxide (24.5% Na_2O) and alkaline earth oxide (24.5% CaO). Such modifier ions are present in network modifying positions and their cations are loosely bound and can be easily detached during leaching ion exchange processes.

In a recent study, Lynch et al. [20] demonstrate by FTIR reflectance spectroscopy that the mechanism of corrosion in lithium disilicate glass occurs primarily by two mechanisms: leaching (ion exchange or dealkalization) and network dissolution. They added that the exact mechanism for aqueous leaching has not been unequivocally determined for all glasses, but the leading theories state that water, in the form of H_3O^+ and/or H_2O, diffuses into the glass according to the proposed equations [21]:

$$\equiv\mathrm{Si{-}OR} + \mathrm{H_3O^+} \rightarrow \equiv\mathrm{Si{-}OH} + \mathrm{R^+} + \mathrm{H_2O} \quad (1)$$

$$\equiv\mathrm{Si{-}OR} + \mathrm{H_2O} \rightarrow \equiv\mathrm{Si{-}OH} + \mathrm{R^+} + \mathrm{OH^-} \quad (2)$$

whereas the suggested reaction for network dissolution is given in Eq. (3):

$$\equiv\mathrm{Si{-}O{-}Si(OH)} + \mathrm{(OH)^-} \rightarrow \equiv\mathrm{Si{-}O{-}Si(OH)_4}^- \rightarrow \equiv\mathrm{Si{-}O^-} + \mathrm{Si(OH)_4} \quad (3)$$

The reaction associated after the formation of SiO_2 gel is the condensation of the Si–OH groups, given in Eq. (4)

$$\mathrm{Si{-}OH} + \mathrm{HO{-}Si} \rightarrow \mathrm{Si{-}O{-}Si} + \mathrm{H_2O} \quad (4)$$

The studied dental glasses consist of multicomponent oxides including silica, lithia, alumina, magnesia, zirconia, potash and P_2O_5. The behavior of such glasses is expected to be different than the previously mentioned traditional commercial glasses and Hench's bioglass although of their common silicate network. The difference in corrosion behaviour can be considered to be due to several possible reasons:

(1) Li^+ ions have relatively smaller ionic radii and can move easily through the suggested percolation channels suggested by Greaves [22] through the diffusion process. However, Li^+ ions possess relatively strong field strength and induce phase separation in glass [1,4] and glasses containing Li_2O are known to be the basic component for the production of glass–ceramics since the early announcement of Stookey [23]. It is also evident that $Li_2O \cdot SiO_2$ glasses can be easily self-nucleated and crystallized without the need of nucleating agents [24,25].
(2) Al_2O_3, MgO and ZrO_2 are known to form structural building groups in the glass which improve the chemical durability. They necessitate nearby attached alkali ions to compensate for surplus electrical neutrality and such alkali ions are tightly bound and cannot be easily detached during the corrosion process. It has been established that the introduction of such oxides as Al_2O_3, MgO or ZrO_2 markedly improve the chemical durability of lithium silicate glass to a measurable degree [26].

4.3. UV–vis absorption properties

Many authors [27,28] have previously assumed that the ultraviolet charge transfer bands usually observed in most commercial glasses are related to unavoidable iron impurities within the raw materials used for glass preparation. Later studies [29–31] have identified the same observation and reached to the same conclusion. Recently, ElBatal et al. have confirmed the presence of the previously established UV charge transfer bands in phosphate [32,33], bioglass [34], cabal [35], borosilicate [36] and Li diborate [37] glasses.

All the present studied glasses reveal pronounced ultraviolet charge transfer absorption bands in the vicinity of 200–300 nm which obviously originate from trace iron impurities and mostly due to Fe^{3+} ions. The observed broadness and marked splitting is related to the possible presence of more than one site of the iron species [35–37].

The appearance of extra charge transfer ultraviolet bands in the glasses containing 10% TiO_2 can be related to the sharing of Ti^{4+} ions. It is known that Ti^{4+} belongs to the d^o configuration which exhibits a charge transfer UV band [38] and the studied glass is believed to favour the tetravalent state of titanium.

4.4. Interpretation of the crystallization data

The nucleation and crystallization kinetics of lithium silicate glasses close to $Li_2O{\cdot}2SiO_2$ (LS_2) composition have been studied intensively for decades because this glass can be made and crystallize easily and detailed thermodynamic data are available in the literature [1,4,24]. Some authors [24,39–41] early assumed that lithium metasilicate phase is formed first as nuclei or droplets and subsequently the main stable lithium disilicate phase is shown to persist. Several authors [42,43] suggested the possibility of a metastable phase (or phases) precipitation in the events of the lithium silicate crystallization. Later studies [44] give some evidence of a lithium metasilicate (LS), which nucleates simultaneously with the stable LS_2 phase. However, there is still some uncertainty over whether metastable phases form and serve as precursors for subsequent precipitation of the stable LS_2 phase, or if the precipitation of the stable phase occurs concurrently and independently of the formation of metastable phases. It is obvious that the sources of this discrepancy come from the glass composition studied, method of glass preparation, condition of melting and heat treatment regime and water content.

The present multicomponent compositions studied consist of various constituent oxides, some of which are considered to induce phase separation in glasses (e.g. MgO, P_2O_5, TiO_2, and ZrO_2) [24,45]. It is therefore suggested that these glasses are expected to possess numerous nucleation sites which promote ease and almost complete crystallization of the glassy products.

5. Conclusion

Chemical behaviour and infrared studies were carried out of some multicomponent lithium silicate based glasses and their glass–ceramic derivatives to investigate their properties and characterize their possible dental application.

Experimental data indicate the interness of the proposed multicomponent glass–ceramics towards all studied leaching solutions. X-ray diffraction patterns reveal the formation of lithium disilicate as a major phase together with other subsidiary phases precipitated during the crystallization process according to the other constituent oxides. Infrared spectra show mainly characteristic bands due to silicate network.

Interpretation of the collected data is carried out on the basis of the relevant structural views on the studied basic glass composition and the current views on the mentioned properties.

References

[1] W. Holand, G. Beall, Glass–Ceramics Technology, American Ceramic Society, Westerville, OH, 2002.

[2] R. Van Noort, Dental ceramics, in: Introduction to Dental Materials, 2nd ed., Mosby, Sheffield, U.K, 2002, pp. 231–246.

[3] M. Scweiger, S. Cramer von Clausburch, W. Holand, V. Rheinberger, Process for preparation of shaped translucent lithium disilicate glass–ceramics products, United States Patent 6,420,288 (issued July 16, 2002).

[4] (a) P.F. James, P.W. McMillan, Phys. Chem. Glasses 11 (1970) 59;
(b) P.F. James, J. Mater. Sci. 10 (1975) 1802.

[5] S. Jayaraman, R.K. Brow, S.T. Reis, E. Apel, N. Rheinberger, W. Holand, J. Am. Ceram. Soc. 90 (3) (2007) 706–711.

[6] R.G. Newton, Glass Technol. 26 (1985) 21–38.

[7] K.M. ElBadry, F.A. Moustaffa, M.A. Azooz, F.H. ElBatal, Glass Technol. 43 (2002) 162–176.

[8] ISO-Standard 6872 Dental Ceramics, 1995 (E) 6.

[9] I. Szabo, B. Nagy, G. Volksch, W. Holland, J. Non-Cryst. Solids 272 (2000) 191–199.

[10] C.I. Merzbacher, W.B. White, J. Non-Cryst. Solids 130 (1991) 18.

[11] H.A. Elbatal, N.A. Ghoneim, N.A. Abdel Shafi, M.A. Azooz, Indian J. Pure Appl. Phys. 38 (2000) 101.

[12] F.H.A. ElBatal, N. Nada, S.M. Desouky, M.M.I. Khalil, Indian J. Pure Appl. Phys. 42 (2004) 711.

[13] J. Zarzycki, Glasses and The Vitreous State, Cambridge University Press, Cambridge, 1991.

[14] J.E. Shelby, Introduction to Glass Science and Technology, Royal Society RSC Press, Cambridge, 1997.

[15] D.E. Clark, C.G. Pantano, L.L. Hench, Corrosion of Glass, Magazines for Industry, New York, 1979.

[16] R.H. Doremus, Glass Science, 2nd edition, John Wiley & Sons, Inc., New York, 1994.

[17] A. Paul, Chemistry of Glasses, 2nd edition, Chapman and Hall, New York, 1990.

[18] L.L. Hench, J. Am. Ceram. Soc. 74 (1991) 1487–1510;
L.L. Hench, J. Am. Ceram. Soc. 81 (1998) 1705–1728.

[19] K.M. ElBadry, F.A. Moustaffa, M.A. Azooz, F.H. ElBatal, Glass Technol. 43 (4) (2002).

[20] M.E. Lynch, D.C. Folz, D.E. Clark, J. Non-Cryst. Solids 353 (2007) 2667–2671.

[21] B.C. Bunker, J. Non-Cryst. Solids 179 (1994) 300.

[22] G.N. Greaves, J. Non-Cryst. Solids 71 (1985) 203.

[23] S.D. Stookey, Glastech. Ber. 32K (1959) 1–8.

[24] W. Vogel, Structure and Crystallization of Glasses, Pergamon Press, Leipzig, 1971.

[25] W. Vogel, Glass Chemistry, 2nd edition, Springer-Verlag, Berlin, 1994.

[26] A.A. Ahmed, N.A. Ghoneim, H.A. ElBatal, F.A. Khalifa, J. Non- Cryst. Solids 41 (1980) 57.

[27] G.H. Sigel, R.J. Ginther, Glass Technol. 9 (1968) 66.

[28] L. Cook, K.H. Mader, J. Am. Ceram. Soc. 65 (1982) 109.

[29] J.A. Duffy, Phys. Chem. Glass. 38 (1997) 289.

[30] D. Ehrt, U. Natura, P. Ebeling, J. Non-Cryst. Solids 263–264 (2000) 240.

[31] D. Moncke, D. Ehrt, Opt. Mater. 25 (2004) 425.

[32] F.H. ElBatal, S.M. AboNaf, F.M. EzzElDin, Indian J. Pure Appl. Phys. 43 (2005) 590.

[33] S.Y. Marzouk, F.H. ElBatal, NIMB 248 (2006) 90.

[34] F.H. ElBatal, S.Y. Marzouk, M.A. Azooz, Phys. Chem. Glass.: Eur. J. Glass Sci. Technol. B 47 (2006) 588.

[35] S.Y. Marzouk, F.H. ElBatal, A.M. Salem, S.M. AboNaf, Opt. Mater. 29 (2007) 1456–1466.

[36] F.H. ElBatal, M.A. Azooz, S.Y. Marzouk, M.S. Selim, Phys. B 398 (2007) 126–134.

[37] F.H. ElBatal, A.A. ElKheshen, M.A. Azooz, S.M. AboNaf, Opt. Mater. 30 (2008) 881–891.
[38] C.R. Bamford, Colour Generation and Control in Glass, Glass Science &Technology, vol. 2, Elsevier, Amsterdam, 1977.
[39] N.A. Ghoneim, H.A. ElBatal, A.A. Ahmed, F.A. Khalifa, Trans. J. Br. Ceram. Soc. 58 (1979) 15–22.
[40] S.W. Freiman, L.L. Hench, J. Am. Ceram. Soc. 51 (1968) 382.
[41] L.L. Hench, S.W. Freiman, D.L. Kinser, Phys. Chem. Glass. 12 (1971) 50.
[42] Y. Iqbal, W.E. Lee, D. Holland, P.F. James, J. Non-Cryst. Solids 224 (1998) 1.
[43] L.L. Burgner, P. Lucas, M.C. Weinberg, P.C. Soares Jr., E.D. Zanotto, J. Non-Cryst. Solids 274 (2000) 188–194.
[44] P.C. Soares Jr., E.D. Zanotto, V.M. Fokin, H. Jain, J. Non-Cryst. Solids 321 (2003) 217–227.
[45] P. Hudon, D.R. Baker, J. Non-Cryst. Solids 303 (2002) 299–345.